PIER M

Design and Analysis of a Low-Profile Tapered Slot UWB Vivaldi Antenna for Breast Cancer Diagnosis

Shanmugam Sasikala[1], Kandasamy Karthika[1], Shanmugam Arunkumar[1], Karunakaran Anusha[1],
Srinivasan Adithya[1], and Ahmed Jamal Abdullah Al-Gburi[2, *]

[1]*Department of Electronics and Communication Engineering*
Kumaraguru College of Technology, Coimbatore, Tamil Nadu 641049, India
[2]*Center for Telecommunication Research & Innovation (CeTRI)*
Fakulti Teknologi dan Kejuruteraan Elektronik dan Komputer (FTKEK)
Universiti Teknikal Malaysia Melaka (UTeM), Jalan Hang Tuah Jaya, Durian Tunggal, Melaka 76100, Malaysia

ABSTRACT: Antennas are significant passive components in Microwave Imaging (MWI) system. The proposed work focuses on the design and analysis of a Vivaldi antenna of size $45 \times 40 \times 1.6\,\mathrm{mm}^3$ for breast cancer diagnosis. The proposed antenna utilizes an FR4 substrate and offers a wideband response. The suggested antenna design is based on a tapered slot antenna. The design utilizes microstrip slot line transition feed as it provides good impedance matching and wide bandwidth. The proposed antenna's design attributes like the radius of the slot and tapering rate are optimized through parametric analysis to achieve desired ultra-wideband (UWB) performance. The UWB offered by the designed antenna is 13.87 GHz (2.79 GHz–16.66 GHz). A Voltage Standing Wave Ratio (VSWR) of less than 2 is obtained for the entire resonating frequency range. The proposed antenna exhibits 60% size reduction compared to the conventional Vivaldi antenna with a peak gain and directivity of 4.77 dBi and 5.84 dBi, respectively. A breast phantom has been designed and simulated for Specific Absorption Rate (SAR) calculation. The designed structure exhibits an average SAR of 0.997 W/kg. Further, the proposed antenna is fabricated and tested. The measured results agree with simulation findings. Hence, the compactness and radiation performance of the proposed antenna makes it suitable for breast cancer diagnosis.

1. INTRODUCTION

The most predominant disease in women is breast cancer. As per the World Health Organization (WHO), there were millions of cases of breast cancer reported across the globe in 2020 leading to 685,000 deaths [1]. The chance of survival is poor in women having breast cancer in later stages (stages III and IV). Patients' survival rates will rise significantly with early identification of breast cancer [2]. Mammography is commonly employed to detect tumors. The disadvantages of mammography include radiation risk and false detection [3, 4]. Microwave imaging system is a promising technology for diagnosing breast cancer [5]. MWI is safer, cost-effective, and more accurate. Here, the microwave signals are sent through the breast tissues, and the reflected signals are received by the antenna at the receiving end. From the received signals, the image can be reconstructed through an efficient image reconstruction algorithm. Thus, in MWI, antenna design and image reconstruction are crucial. Antenna design and its characteristics in MWI can affect the quality of the image produced. The use of electromagnetics in MWI to diagnose breast cancer is discussed in [2, 6, 7].

Designing antennas for the MWI should meet the following requirements: wide bandwidth, high gain, small size factor, and low SAR values. The significance of UWB in the diagnosis of breast cancer is analyzed and experimented in [8, 9]. Due to wide impedance bandwidth scanning may be performed throughout a wider frequency spectrum, resulting in images with significantly improved contrast surrounding the tumor [10]. The design of a UWB slotted monopole operating from 3.1 GHz to 10.6 GHz is presented in [11]. The designed structure has been optimized to achieve high bandwidth and gain. Improved frequency response through a Coplanar Vivaldi Antenna (CVA) is analyzed [12]. This antenna works from 1.3 GHz to 7.09 GHz. The design approach was initiated by designing a conventional coplanar Vivaldi antenna. In the size-reduced structure, directors are placed along the flare opening region to enhance directivity and bandwidth. A wearable bra with a UWB Multiple Input Multiple Output (MIMO) antenna operating from 4.8 to 30 GHz is experimented in [13]. The radiating part is an antipodal Vivaldi antenna, and it offers circular polarization and an improved directional pattern.

The detection of breast cancer using 4×4 antenna arrays operating between 2 and 4 GHz is presented in [14]. Here, each antenna is a spiral antenna and radiates 1 mW of power. The antenna array exhibits an efficiency of 95.6% and a gain of 17 dBi. The UWB MIMO antenna for breast cancer diagnosis is designed and discussed [15]. The upper part containing the circular patch is responsible for UWB. The metasurface loaded as a superstrate over a triangular-shaped antenna

---

* Corresponding author: Ahmed Jamal Abdullah Al-Gburi (ahmedjamal@ieee.org, ahmedjamal@utem.edu.my).
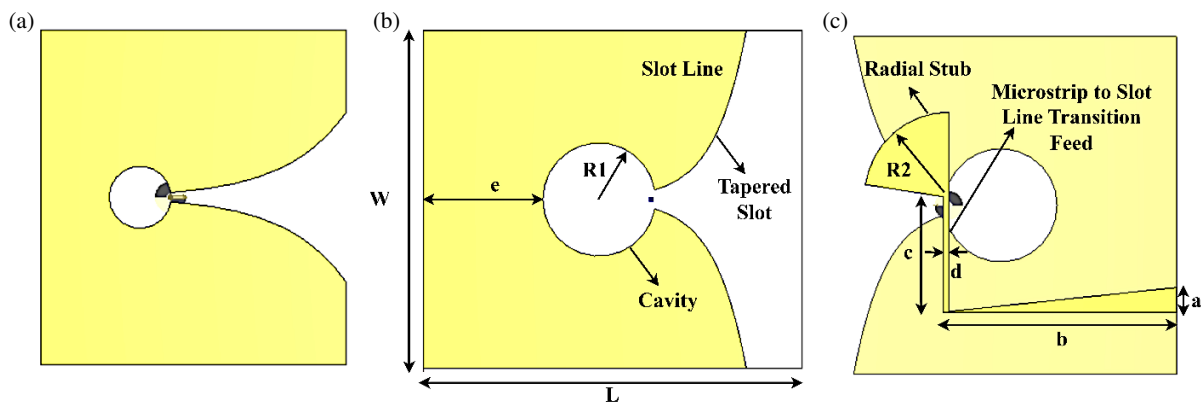
FIGURE 1. UWB Vivaldi antenna design for breast cancer diagnosis. (a) Initial design — Conventional Vivaldi antenna. (b) Proposed design — Front view. (c) Proposed design — Back view. ($L = 45$ mm, $W = 40$ mm, $R1 = 6.5$ mm, $R2 = 10$ mm, $a = 3$ mm, $b = 27.1$ mm, $c = 13.7$ mm, $d = 0.6$ mm, $e = 14.22$ mm, tapering rate $= 0.265$).

is presented to improve the radiation efficiency and transmission parameters [16]. Metasurface loaded in the opening region of the Vivaldi antenna offers high gain [17]. The addition of slots in the sides of the Vivaldi antenna excites the higher order modes which increase the gain and directivity of the antenna [18]. Metasurface can also be used to enhance the bandwidth and reduce SAR in MWI antennas [19]. The design of microwave imaging antennas should consider mutual coupling reduction and isolation enhancement since they can greatly improve the efficiency and precision of the imaging system. This can be realized by incorporating methods inspired by metamaterials and metasurfaces [20–22]. Antenna array having high isolation can accommodate more antennas to get high resolution images. A metamaterial inspired antenna array has been designed for tumor detection in breasts. This antenna can exhibit wide impedance bandwidth without increasing its physical size [10]. For breast cancer detection, Artificial Intelligence (AI) assisted algorithms can be utilized to identify the malignant tumor [23]. For on-body wearable applications, the antenna can utilize wearable substrate materials [24, 25] and/or copper coated conductive fabric as a patch [26]. Further, analyzing the effects of bending makes it suitable for conformal applications [27].

According to the literature survey, several research studies have been undertaken by researchers to develop a highly efficient antenna for MWI. This paper aims to design and analyze a Vivaldi antenna as it offers a wide bandwidth and is appropriate for breast cancer diagnosis. The key contributions of this work are listed as follows:

- A compact Vivaldi antenna design is designed and analyzed.
- In addition to performance enhancement through parametric analysis, the work focuses on size reduction by altering the design attributes. This is a significant value addition of the proposed work to the works existing in literature.
- Breast phantom is designed to measure SAR.

In this work, Section 2 discusses the design procedure of the proposed Vivaldi antenna design. The simulation findings are discussed in Section 3. Section 4 concludes the paper.

2. ANTENNA DESIGN FOR BREAST CANCER DIAGNOSIS

2.1. Antenna Design

The proposed research work focuses on designing a Vivaldi antenna that can cover UWB frequencies. FR4 substrate has a low loss tangent which helps to minimize signal attenuation at microwave frequencies. While FR4 may not have the superior electrical properties of some other high-frequency substrates, its cost-effectiveness, ease of processing, and mechanical stability make it a popular and practical choice for microwave applications. Hence, an FR4 substrate (dielectric constant of 4.3) of height 1.6 mm is utilized for this proposed design. The size of the designed antenna is $45 \times 40 \times 1.6$ mm^3. A microstrip-to-slot line transition feed is used to connect a microstrip transmission line to a slot antenna.

The proposed Vivaldi antenna along with its design specifications is illustrated in Figures 1(b) and (c). It comprises a cavity, slot line, exponential tapered slot line (flare), and microstrip to transition line feed. The cavity's structure, tapering rate, placement of the stub, and position of the feedline and slots determine the Vivaldi antenna's radiation characteristics. A cavity with a radius $R1$ is present at the flare's end. The radius of the circular cavity can be approximated by $\lambda_a/4$ where λ_a is the effective wavelength of the slot line [28]. The microstrip to slot line feed on the other side of the substrate excites the circular cavity. The circular cavity minimizes the reflections from the feed and transfers the energy to the tapered slot line. The Vivaldi antenna's primary radiating element is controlled by a flare. Flare is characterized using its height, length, and tapered rate. The exponential tapered slot line (flare), along which the wave is radiated, is referred to as the radiation section. The tapered slot provides broadband characteristics by allowing radiation at various frequencies. The exponential taper is defined using Equation (1) [29, 30]:

$$y = \pm Ce^{rx} \quad (1)$$

where C is a constant, 'r' the tapering rate, and 'x' the position along the length of the taper slot. Using the following Equation (2), the Vivaldi antenna's resonance or cut-off frequency
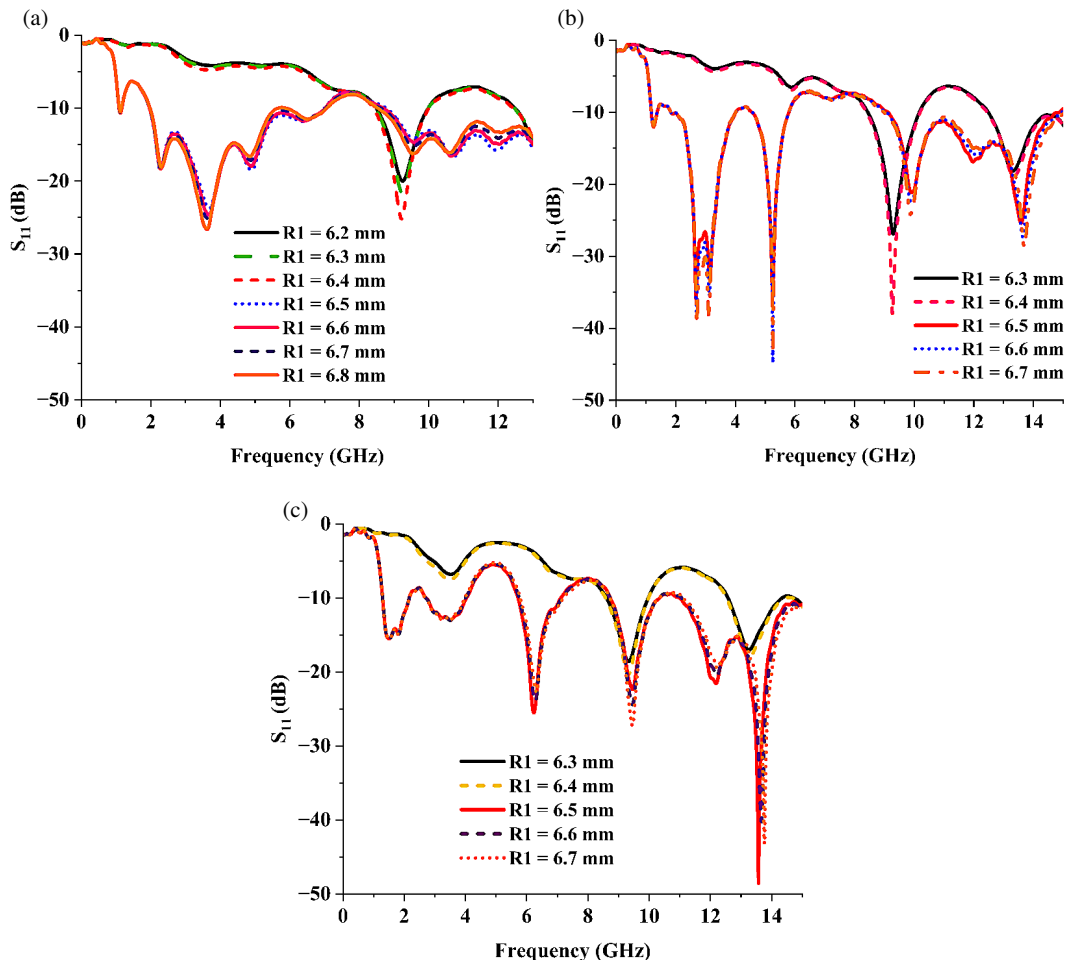
FIGURE 2. Parametric analysis of various cavity radius ($R1$) with length L, (a) $L = 64$ mm, (b) $L = 54$ mm, (c) $L = 45$ mm.

can be obtained.

$$f_c = \frac{c}{w'\sqrt{\varepsilon_r}} \qquad (2)$$

where $c = 3 \times 10^8$ m/s; f_c indicates the center frequency; the substrate's relative permittivity is ε_r; and w' denotes the flare edge's width opening. w' can also be approximated using (3).

$$w_1 < w' < w_2 \qquad (3)$$

where $w_1 \approx \lambda_o$ (at $f_c = 6.85$ GHz); $w_2 \approx \lambda_{\min}/2$ (at $f_L = 3.1$ GHz) [31].

A microstrip to slot line transition feed has been utilized in this Vivaldi antenna design. Antenna excitation occurs due to electromagnetic coupling. A tapered microstrip feed is properly designed for $50\,\Omega$ input impedance. The length of the microstrip feed line (b) nearly equals half the antenna's length (L) added to $R2/2$, and width of the microstrip line is tapered to match the impedance of the slot line and the feed line. A 90° radial stub is connected to the microstrip feed's end to broaden the bandwidth of the antenna for impedance matching. The radius of the radial stub can be approximated by $\lambda_r/4$ where λ_r denotes the microstrip feed's effective wavelength. The initial work proceeds with the calculated values obtained using Equations (1) and (2). The design has a tapering rate of 0.078, cavity radius of 6.5 mm, flare opening width of 35.56 mm, aperture length of 37 mm, and radial stub radius of 10 mm. The overall dimension of the initially designed antenna depicted in Figure 1(a) is $64 \times 70 \times 1.6$ mm^3. This design results in a wide bandwidth of 5.12 GHz (1.94 GHz–7.06 GHz). The obtained VSWR for the entire -10 dB bandwidth is around 1.9, and the overall gain is 2.52 dBi. The obtained performance of the initially designed antenna is not sufficient for MWI applications. Further, the size of the antenna can be reduced for easy implementation in the MWI system.

2.2. Parametric Analysis

To improve the antenna's bandwidth, parametric analysis has been done for cavity radius ($R1$) and tapering rate (r). Additionally, to achieve a compact structure, the antenna's width (W) and length (L) were also modified. Firstly, the width of the antenna was optimized to 40 mm for optimal performance. Then the parametric analysis was done with $L = 64$ mm, 54 mm, and 45 mm for varied values of $R1$. Comparing the simulation findings represented in Figure 2, the cavity with a radius of 6.5 mm for $L = 45$ mm offers better performance with reduced size. Further, the parametric analysis has been carried out for various tapering rates with $L = 54$ mm, keeping 6.5 mm as the cavity radius.
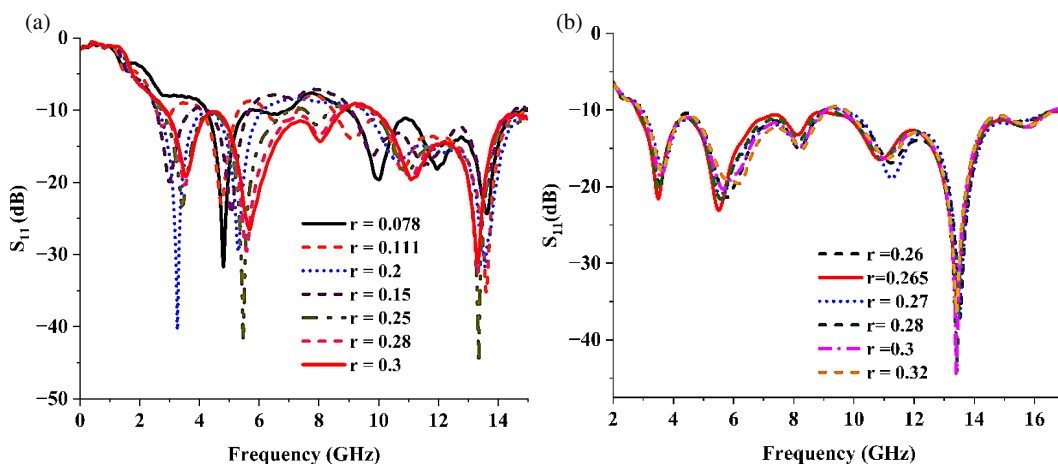
FIGURE 3. Parametric analysis of different tapering rates (r) with length, (a) $L = 54$ mm, (b) $L = 45$ mm.
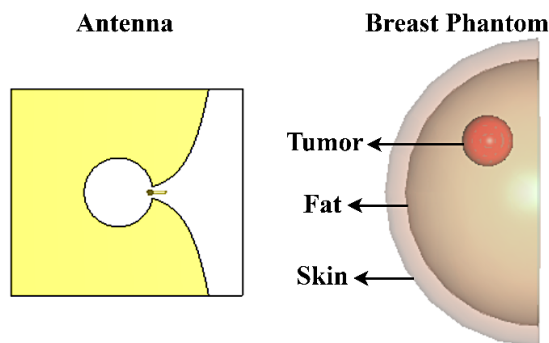

FIGURE 4. Modeled breast phantom for SAR calculation.

FIGURE 5. S_{11} plot of the proposed Vivaldi antenna vs initial design.

According to Figure 3(a), wide bandwidth is observed for a tapering rate of 0.3. The size is further reduced by changing L to 45 mm, and a parametric sweep has been performed for various tapering rates. According to the simulation findings in Figure 3, the tapering rate (r) of 0.265 provides ultra-wide bandwidth coverage with acceptable performance. Thus, the proposed antenna of size 45×40 mm^2 with tapering rate 0.265 and circular cavity radius 6.5 mm is achieved through parametric analysis. This results in a size reduction about 60% compared to the conventional Vivaldi antenna design.

2.3. Breast Phantom for SAR Analysis

In breast cancer diagnosis, breast cancer tissue can be characterized by its dimensions in terms of size, shape, and location within the breast. The dimensions of breast cancer tissue are important for diagnosis, staging, and treatment planning. The size of breast cancer tissue is usually measured in three dimensions: length, width, and depth. Breast tumors can be round, oval, irregular, or lobulated. The breast phantom comprises skin layer, fat layer, and breast tumor. Table 1 summarizes the properties of breast tissue [32].

While designing antennas for microwave imaging, it is important to consider the SAR. SAR describes the amount of
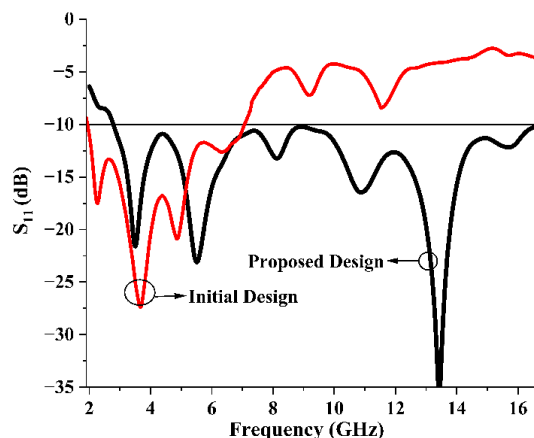
TABLE 1. Breast tissue — Dielectric properties [32].

Tissue	Density (kg/m^3)	Permittivity (F/m)	Electrical Conductance (S/m)
Tumor	1058	54.9	4
Fat	911	4.84	0.262
Skin	1109	36.7	2.34

power absorbed by the tissue. As per safety regulations, the SAR threshold value is 1.6 W/kg. The human breast can be modeled into a phantom by using its dielectric properties to examine the SAR of the designed antenna. For analysis purposes, a round-shaped breast tumor of diameter 10 mm is chosen and positioned at $(x, y, z) = (41, 10, 10)$ [dimensions in mm] arbitrarily. The designed breast phantom is located along the direction of the main lobe. The modeled breast phantom along with the designed antenna is illustrated in Figure 4.

3. RESULTS AND DISCUSSION

A UWB Vivaldi antenna is modeled, and its simulation performances are discussed in this section. Radiation properties in-
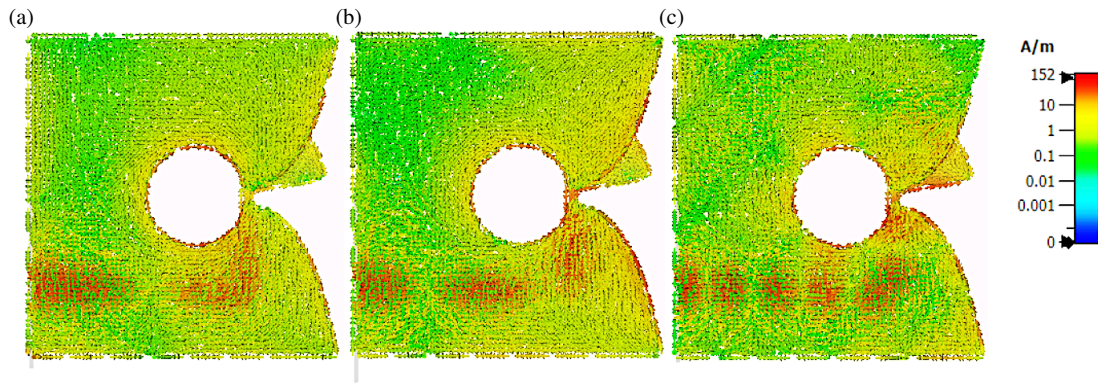
FIGURE 6. Surface current distribution, (a) 3.5 GHz, (b) 5.5 GHz, (c) 13.43 GHz.
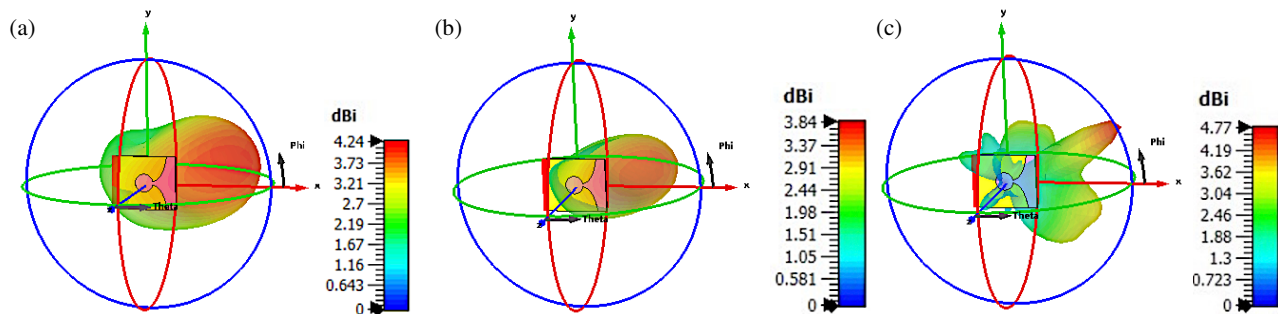

FIGURE 7. Simulated gain — 3D plot, (a) 3.5 GHz, (b) 5.5 GHz, (c) 13.43 GHz.

cluding S_{11}, gain, VSWR, and radiation pattern have been examined in the simulation. Figure 5 depicts the S_{11} comparison between the initial antenna design and the final design. The initial structure covers the frequencies from 1.94 GHz to 7.6 GHz whereas the proposed structure provides ultra-wide bandwidth operating from 2.79 GHz to 16.66 GHz. Compared to the initial design, the proposed structure offers an increased bandwidth of 8.92 GHz. The proposed antenna exhibits a fractional bandwidth of 143%, resulting in a 26% higher value than the initial design. This has been accomplished by changing the cavity's radius and the exponential slot section's tapering rate.

Figure 6 illustrates the surface current distribution. High current distribution is noted along the edges of the radiation section, cavity, and microstrip feed. This implies the energy coupling from the feed to the slot antenna through the cavity and is further transferred to the radiation section. Also, dense current distribution is observed with the increase in frequency. Gain of the proposed antenna at different resonant frequencies is shown in Figure 7. 4.24 dBi, 3.84 dBi, and 4.77 dBi are the simulated gains observed at 3.5 GHz, 5.5 GHz, and 13.43 GHz, respectively. SAR analysis is significant while designing an antenna for biomedical or wearable application. SAR can be calculated using Equation (4).

$$\text{SAR}_{\text{average}}(r, \omega) = \frac{1}{v} \int \frac{\sigma(r, \omega) \, |E(r, \omega)|_2}{2\rho(r)} \, dr \qquad (4)$$

where 'v' denotes the volume [m^3]; $\sigma(r, \omega)$ represents tissue conductivity (S/m); $\rho(r)$ indicates the tissue's mass density at

'r' [kg/m^3]; and $E(r, \omega)$ represents the electric field strength within the tissue [V/m].

Using CST, the SAR calculations are performed for 10 gram of mass tissue at all three resonating frequencies (3.5 GHz, 5.5 GHz, 13.43 GHz) in the UWB coverage. From Figure 8, it is observed that SAR achieved at 3.5 GHz, 5.5 GHz, and 13.43 GHz are 0.45 W/kg, 1.26 W/kg, and 1.28 W/kg respectively. In SAR analysis, the location having maximum SAR can be identified as the tumor's estimated position [33]. The positions $(x, y, z) = (43.1872, 13.0841, 12.7495)$, $(43.2454, 14.7323, 13.2331)$, and $(43.9454, 13.6218, 14.2232)$ are the estimated positions of the tumor at 3.5 GHz, 5.5 GHz, and 13.43 GHz, respectively. The actual tumor and the estimated tumor at all the resonating frequencies are illustrated in Figure 9. It is detected that the predicted tumor is located almost nearer to the actual tumor. While designing antenna for microwave imaging, SAR value of the antenna gives information on amount of energy being absorbed by the tissue. This can be used to make sure that the energy levels of the radiation are safe and do not endanger the patient's health. In literature, SAR value is utilized in simulation analysis to estimate the location of the tumor. However, in the real time implementation, SAR is not directly related to tumor detection. The proposed antenna should be placed near the breast to transmit electromagnetic waves through it. During penetration, the electromagnetic (EM) waves will interact with the respective tissues and tumors if any. The antenna detects the reflected and or scattered signals from the tumors. Then, the detected signals are processed using microwave imaging algorithms to accurately create the
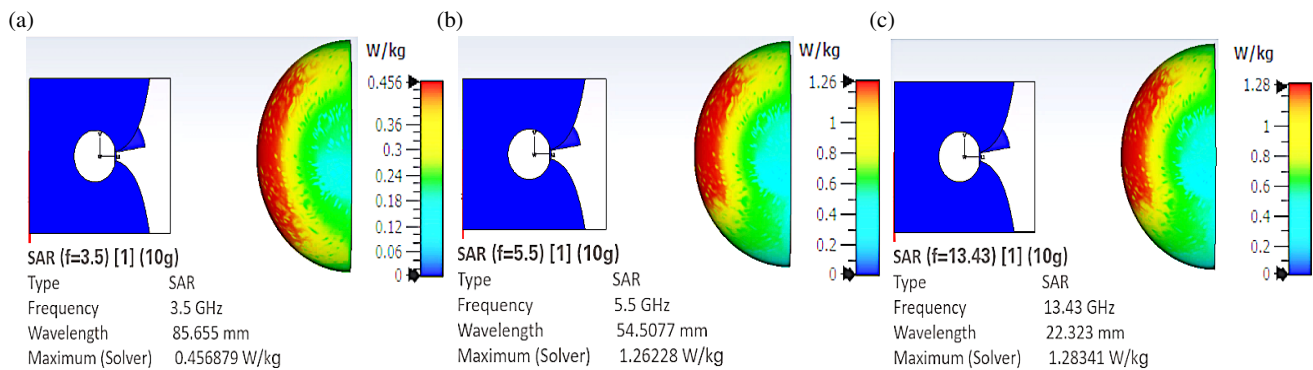
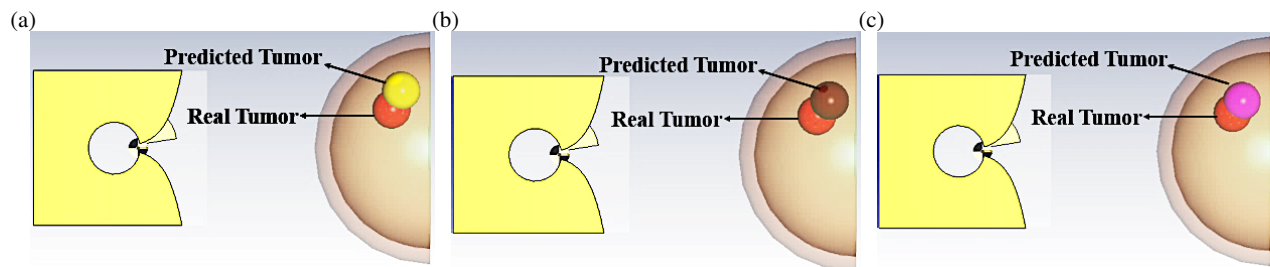**FIGURE 8**. SAR, (a) 3.5 GHz, (b) 5.5 GHz, (c) 13.43 GHz.

FIGURE 9. Actual tumor vs predicted tumor, (a) 3.5 GHz, (b) 5.5 GHz, (c) 13.43 GHz.
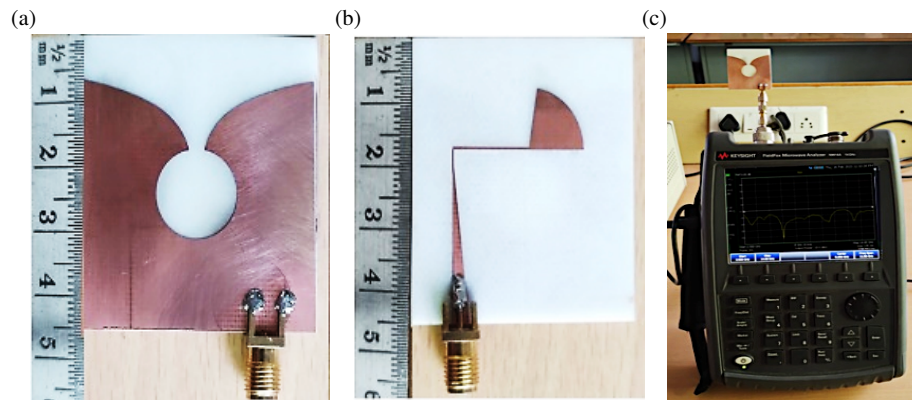

FIGURE 10. Fabricated antenna, (a) front view, (b) back view, (c) vector network analyzer measurement setup for testing the proposed antenna.

tumor image and estimate its location. This can be done in the future work to assess the efficacy of the proposed structure.

The proposed antenna is fabricated and tested to validate its performance. The front and rear views are shown in Figures 10(a) and (b), respectively. Figure 10(c) shows the VNA measurement setup to measure the antenna's S_{11} and VSWR.

The measured S_{11} and VSWR of the designed structure are compared with the simulation findings and depicted in Figures 11(a) and (b), respectively. The S_{11} measured result shows the resonance at 3.4 GHz, 5.75 GHz, 9.6 GHz, and 12 GHz. VSWR value of less than 2 is observed for the measured bandwidth (8.2 GHz). Moreover, the measured bandwidth is comparatively low compared to the simulated bandwidth. This variation in measured results might have happened due to an error during the fabrication process or antenna alignment or

positioning error during the measurement process. The radiation pattern of the fabricated antenna has been measured at 3.4 GHz, 5.75 GHz, and 12 GHz. Figure 12 compares the radiation pattern of measured and simulated results in Phi = 0° and Phi = 90°. The radiation pattern is observed along the direction of the flare's opening. At Phi = 0°, the main lobe direction is observed along +90° in all the resonating frequencies. When Phi = 90°, the main lobe is observed along the directions +30°, +30°, +150° for 3.4 GHz, 5.75 GHz, and 12 GHz, respectively. The mild variations is observed between the simulated and measured radiation pattern results owing to measurement setup.

The proposed design's simulation findings have been compared with a few existing works in literature and listed in Table 2. The proposed antenna offers wider bandwidth
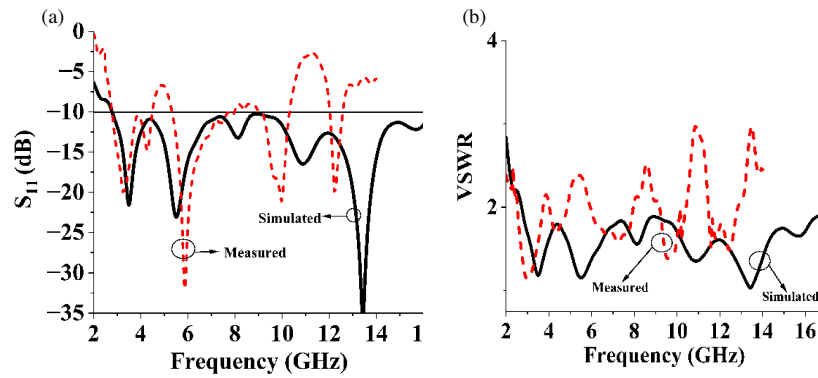
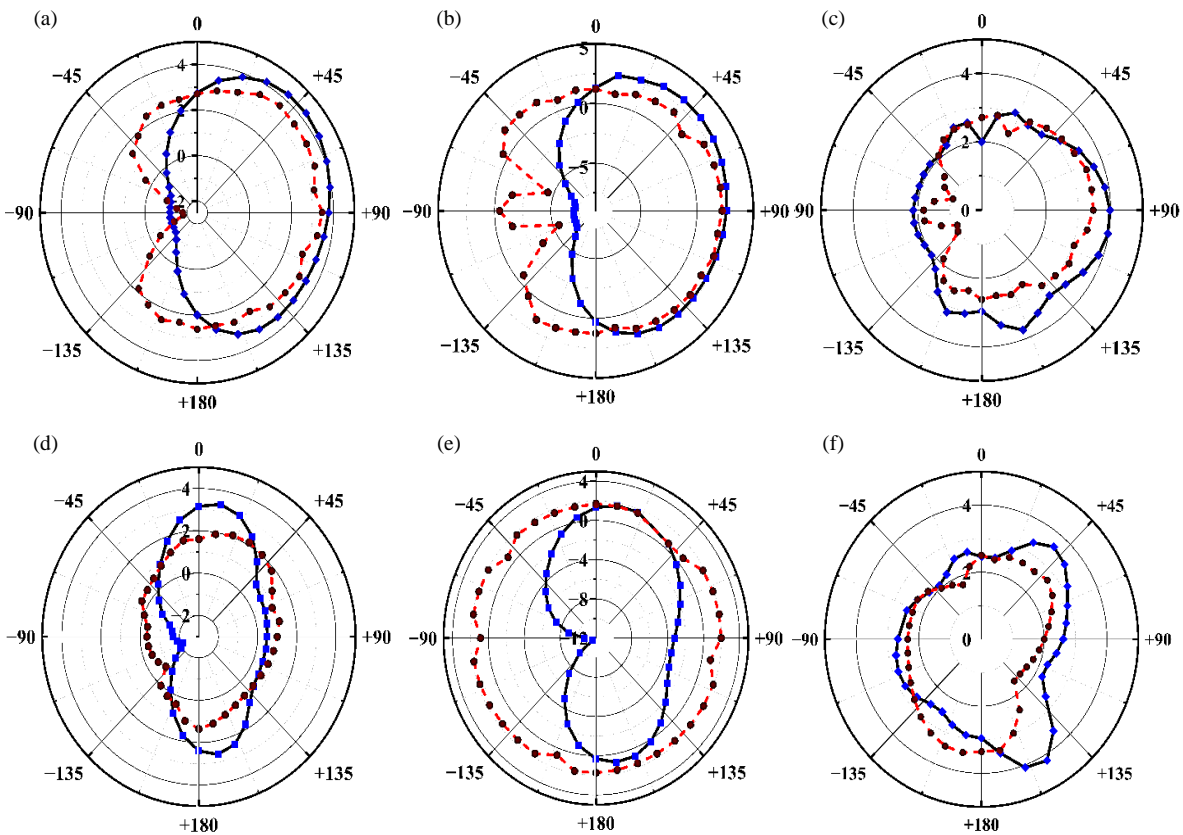**FIGURE 11**. Simulation vs measured results, (a) return loss, (b) VSWR.

FIGURE 12. Radiation pattern: Phi = 0, (a) 3.4 GHz, (b) 5.75 GHz, (c) 12 GHz; Phi = 90, (d) 3.4 GHz, (e) 5.75 GHz, (f) 12 GHz.

TABLE 2. Results comparison with existing works.

Ref. No.	Substrate	UWB Frequency Range (GHz)	Peak Gain (dBi)	Directivity (dBi)	SAR (W/kg)	Design Complexity
[5]	FR-4	6–14	5.8	-	-	Simple
[11]	FR-4	3.1–10.6	4.74	-	2	Medium
[12]	FR4	1.3–7.09	-	9.02	-	Medium
[14]	FR4	2–4	17.4	17.78	-	High
[33]	FR-4	1.6–10	4.431	5.197	0.694	Simple
[34]	FR-4	3.3–10.6	3.49	-	1.19	Simple
This Work	FR4	2.79–16.66	4.77	5.84	0.997	Medium

than [5, 11, 12, 14, 33, 34]. It exhibits lower SAR than [11, 34]. The design complexity mentioned in Table 2 is based on the number of parameters involved in the design and its structural geometry. The proposed complexity of the proposed antenna is lower than [11, 12, 14]. The realized peak gain of the designed antenna is higher than [11, 33, 34].

4. CONCLUSION

This work proposes a compact Vivaldi antenna design for breast cancer diagnosis. In this design, the radius of the cavity and tapering rate of the exponential slot section are altered for UWB coverage and size reduction. SAR calculation is done by creating a breast phantom using CST simulation software. The proposed antenna offers UWB coverage of 13.87 GHz with VSWR less than 2. The peak gain of the proposed antenna is 4.77 dBi, and its efficiency is 76.7%. The average SAR value offered by the proposed antenna is 0.997 W/kg. The proposed Vivaldi antenna offers size reduction by 60% and improved bandwidth by 171% compared to the initial design. The designed antenna exhibits improved performances w.r.t ultra-wideband coverage, a small size factor, and low SAR values. Further, at all the resonating frequencies, the estimated position of the tumor is close to the actual tumor. Hence, the suggested antenna can be utilized in microwave imaging techniques for efficient breast cancer diagnosis. Fabrication and testing are done to validate the antenna's performance. Minor deviation is observed in the measured result. The gain of the designed structure can be improved further by implementing metamaterials or metasurfaces or antenna arrays in future work.

ACKNOWLEDGEMENT

REFERENCES

[1] World Health Organization, "Breast cancer fact sheets," https://www.who.int/news-room/fact-sheets/detail/breast-cancer, 2021.

[2] Khalil, M. H., J. D. Xu, and T. Tumenjargal, "Microwave imaging: Potential for early breast cancer detection," *Proceedings of the Pakistan Academy of Sciences*, Vol. 49, No. 4, 279–288, 2012.

[3] Heywang-Köbrunner, S. H., A. Hacker, and S. Sedlacek, "Advantages and disadvantages of mammography screening," *Breast Care*, Vol. 6, No. 3, 199–207, 2011.

[4] American Cancer Society, "Limitations of mammograms," https://www.cancer.org/cancer/types/breast-cancer/screening-tests-and-early-detection/mammograms/limitations-of-mammograms.html#written_by, 2017.

[5] Chowdhury, N. A., L. Wang, M. S. Islam, L. Gu, and M. Kaya, "Microstrip patch antenna with an inverted T-type notch in the partial ground for breast cancer detections," *Computer Modeling in Engineering & Sciences*, Vol. 138, No. 2, 1301–1322, 2024.

[6] Zerrad, F.-E., M. Taouzari, M. E. Mostafa, J. E. Aoufi, S. D. Qanadli, M. Karaaslan, A. J. A. Al-Gburi, and Z. Zakaria, "Mi-

crowave imaging approach for breast cancer detection using a tapered slot antenna loaded with parasitic components," *Materials*, Vol. 16, No. 4, 1496, Feb. 2023.

[7] Moloney, B. M., P. F. McAnena, S. M. A. Elwahab, A. Fasoula, L. Duchesne, J. D. G. Cano, C. Glynn, A. M. O'Connell, R. Ennis, A. J. Lowery, and M. J. Kerin, "Microwave imaging in breast cancer — Results from the first-in-human clinical investigation of the wavelia system," *Academic Radiology*, Vol. 29, No. 3, S211–S222, Jan. 2022.

[8] Hassan, A. M. and M. El-Shenawee, "Review of electromagnetic techniques for breast cancer detection," *IEEE Reviews in Biomedical Engineering*, Vol. 4, 103–118, 2011.

[9] Pan, J., "Medical applications of ultra-wideband (UWB)," *Survey Paper*, 2007.

[10] Alibakhshikenari, M., B. S. Virdee, P. Shukla, N. O. Parchin, L. Azpilicueta, C. H. See, R. A. Abd-Alhameed, F. Falcone, I. Huynen, T. A. Denidni, and E. Limiti, "Metamaterial-inspired antenna array for application in microwave breast imaging systems for tumor detection," *IEEE Access*, Vol. 8, 174 667–174 678, 2020.

[11] Danjuma, I. M., M. O. Akinsolu, C. H. See, R. A. Abd-Alhameed, and B. Liu, "Design and optimization of a slotted monopole antenna for ultra-wide band body centric imaging applications," *IEEE Journal of Electromagnetics, RF and Microwaves in Medicine and Biology*, Vol. 4, No. 2, 140–147, Jun. 2020.

[12] Uyanik, C., A. O. Ertay, S. Dogu, I. Akduman, and H. Sahinturk, "A coplanar Vivaldi antenna design with improved frequency response for microwave breast imaging," in *2016 IEEE Conference on Antenna Measurements & Applications (CAMA)*, Syracuse, NY, USA, Oct. 2016.

[13] Mahmood, S. N., A. J. Ishak, A. Jalal, T. Saeidi, S. Shafie, A. C. Soh, M. A. Imran, and Q. H. Abbasi, "A BRA monitoring system using a miniaturized wearable ultra-wideband MIMO antenna for breast cancer imaging," *Electronics (Switzerland)*, Vol. 10, No. 21, Nov. 2021.

[14] Vijaykumar, K., M. Baskaran, V. Gayathri, and P. Gayathri, "Design of 4×4 antenna array for breast cancer detection," *Analog Integrated Circuits and Signal Processing*, Vol. 105, No. 3, 395–406, 2020.

[15] Wang, L. and B. Huang, "Design of ultra-wideband MIMO antenna for breast tumor detection," *International Journal of Antennas and Propagation*, Vol. 2012, 2012.

[16] Ghavami, N., E. Razzicchia, O. Karadima, P. Lu, W. Guo, I. Sotiriou, E. Kallos, G. Palikaras, and P. Kosmas, "The use of metasurfaces to enhance microwave imaging: Experimental validation for tomographic and radar-based algorithms," *IEEE Open Journal of Antennas and Propagation*, Vol. 3, 89–100, 2022.

[17] Islam, M. T., M. Samsuzzaman, S. Kibria, N. Misran, and M. T. Islam, "Metasurface loaded high gain antenna based microwave imaging using iteratively corrected delay multiply and sum algorithm," *Scientific Reports*, Vol. 9, No. 1, 1–14, Nov. 2019.

[18] Islam, M. T., M. Z. Mahmud, M. T. Islam, S. Kibria, and M. Samsuzzaman, "A low cost and portable microwave imaging system for breast tumor detection using UWB directional antenna array," *Scientific Reports*, Vol. 9, No. 1, 1–13, Oct. 2019.

[19] Cai, M., X. Li, L. Fan, G. Yang, and S. K. Sharma, "Broadband compact CPW-fed metasurface antenna for SAR-based portable imaging system," *International Journal of RF and Microwave Computer-Aided Engineering*, Vol. 28, No. 2, 1–9, Feb. 2018.

[20] Koma'rudin, N. A., Z. Zakaria, A. A. Althuwayb, H. Lago, H. Alsariera, H. Nornikman, A. J. A. Al-Gburi, and P. J. Soh, "Directional wideband wearable antenna with circular parasitic

element for microwave imaging applications," *Computers, Materials & Continua*, Vol. 72, No. 1, 983–998, 2022.

[21] Al-Gburi, A. J. A., I. B. M. Ibrahim, M. Y. Zeain, and Z. Zakaria, "Compact size and high gain of CPW-fed UWB strawberry artistic shaped printed monopole antennas using FSS single layer reflector," *IEEE Access*, Vol. 8, 92 697–92 707, 2020.

[22] Alibakhshikenari, M., B. S. Virdee, P. Shukla, C. H. See, R. A. Abd-Alhameed, F. Falcone, K. Quazzane, and E. Limiti, "Isolation enhancement of densely packed array antennas with periodic MTM-photonic bandgap for SAR and MIMO systems," *IET Microwaves, Antennas & Propagation*, Vol. 14, No. 3, 183–188, Mar. 2019.

[23] Elsheakh, D. N., R. A. Mohamed, O. M. Fahmy, K. Ezzat, and A. R. Eldamak, "Complete breast cancer detection and monitoring system by using microwave textile based antenna sensors," *Biosensors (Basel)*, Vol. 13, No. 1, 87, Jan. 2023.

[24] Jayalakshmi, J. and S. Ramesh, "Compact fractal wearable antenna for wireless body area communications," *Telecommunications and Radio Engineering*, Vol. 79, No. 1, 71–80, 2020.

[25] Vanitha, M., S. Ramesh, and S. Chitra, "Wearable antennas for remote health care monitoring system using 5G wireless technologies," *Telecommunications and Radio Engineering*, Vol. 78, No. 14, 1275–1285, 2019.

[26] Annalakshmi, T. and S. Ramesh, "Wearable Panda-shaped textile antenna with annular ring-defected ground structure for wireless body area networks," *Applied Computational Electromagnetics Society Journal*, Vol. 37, No. 5, 546–553, May 2022.

[27] Annalakshmi, T. and S. Ramesh, "Performance and analysis of UWB aesthetic pattern textile antenna for WBAN applica-

tions," *Applied Computational Electromagnetics Society Journal*, Vol. 35, No. 12, 1525–1531, Dec. 2020.

[28] Sarkar, C., "Some parametric studies on Vivaldi antenna," *International Journal of u- and e- Service, Science and Technology*, Vol. 7, No. 4, 323–328, 2014.

[29] Ebnabbasi, K., D. Busuioc, R. Birken, and M. Wang, "Taper design of Vivaldi and co-planar tapered slot antenna (TSA) by Chebyshev transformer," *IEEE Transactions on Antennas and Propagation*, Vol. 60, No. 5, 2252–2259, May 2012.

[30] Pandey, G. K., H. S. Singh, P. K. Bharti, A. Pandey, and M. K. Meshram, "High gain Vivaldi antenna for radar and microwave imaging applications," *International Journal of Signal Processing Systems*, Vol. 3, No. 1, 35–39, 2014.

[31] Saleh, S., W. Ismail, I. S. Z. Abidin, M. H. Jamaluddin, M. H. Bataineh, and A. S. Alzoubi, "Compact UWB Vivaldi tapered slot antenna," *Alexandria Engineering Journal*, Vol. 61, No. 6, 4977–4994, Jun. 2022.

[32] Bah, M. H., J. Hong, D. A. Jamro, J. J. Liang, and E. A. Kponou, "Vivaldi antenna and breast phantom design for breast cancer imaging," in *2014 7th International Conference on Biomedical Engineering and Informatics*, 90–93, Dalian, China, Oct. 2014.

[33] Al Omairi, A. and D. C. Atilla, "Ultra-wide-band microstrip patch antenna design for breast cancer detection," *Electrica*, Vol. 22, No. 1, 41–51, Jan. 2022.

[34] Mathur, M., H. Nigam, D. Mathur, G. Singh, S. K. Bhatnagar, and M. Arora, "Design of wearable UWB microstrip patch antenna for breast cancer tumor detection," *Annals of the Romanian Society for Cell Biology*, Vol. 25, No. 3, 7751–7759, 2021.